^{18}F-Labeling and evaluation of novel MDL 100907 derivatives as potential 5-HT2A antagonists for molecular imaging

Fabian Debus[a],[*],[1], Matthias M. Herth[b],[1], Markus Piel[b], Hans-Georg Buchholz[c],
Nicole Bausbacher[c], Vasko Kramer[b], Hartmut Lüddens[a], Frank Rösch[b]

[a]Clinical Research Group, Department of Psychiatry, Johannes Gutenberg University-Mainz, Untere Zahlbacher Straße 8, 55131 Mainz, Germany
[b]Institute of Nuclear Chemistry, Johannes Gutenberg University-Mainz, Fritz-Strassmann-Weg 2, 55128 Mainz, Germany
[c]Department of Nuclear Medicine, Johannes Gutenberg University-Mainz, Langenbeckstraße 1, 55131 Mainz, Germany

Abstract

Introduction: The serotonergic system, especially the 5-HT2A receptor, is involved in various diseases and conditions. It is a very interesting target for medicinal applications.
Methods: Two novel 5-HT2A tracers, namely, [^{18}F]DD-1 and the enantiomeric pure (R)-[^{18}F]MH.MZ, were radiolabeled by ^{18}F-fluoroalkylation of the corresponding desmethyl analogue. In vitro binding autoradiography on rat brain slices was performed to test the affinity and selectivity of these tracers. Moreover, first μPET experiments of (R)-[^{18}F]MH.MZ were carried out in Sprague-Dawley rats.
Results: [^{18}F]DD-1 (K_i=3.23 nM) and (R)-[^{18}F]MH.MZ (K_i=0.72 nM) were ^{18}F-fluoroalkylated by the secondary synthon [^{18}F]FETos in a radiochemical yield (RCY) of >70%. The final formulation for both tracers took no longer than 100 min with an overall RCY of ~40%. It provided [^{18}F]tracers with a purity >96% and a typical specific activity of 25–35 GBq/μmol. Autoradiographic images of (R)-[^{18}F]MH.MZ (**5**) and [^{18}F]DD-1 (**4**) showed excellent visualization and selectivity of the 5-HT2A receptor for (R)-[^{18}F]MH.MZ and less specific binding for [^{18}F]DD-1. The binding potential (BP) of (R)-[^{18}F]MH.MZ was determined to be 2.6 in the frontal cortex and 2.2 in the cortex (n=4), whereas the cortex-to-cerebellum ratio was determined to be 3.2 at steady state (n=4). Cortex-to-cerebellum ratios of (R)-[^{18}F]MH.MZ were almost twice as much as compared with the racemic [^{18}F]MH.MZ. Thereby, equal levels of specific activities were used. High uptake could be demonstrated in cortex regions.
Conclusion: Labeling of both novel tracers was carried out in high RCY. Autoradiography revealed (R)-[^{18}F]MH.MZ as a very selective and affine 5-HT2A tracer (K_i=0.72 nM), whereas [^{18}F]DD-1 showed no reasonable distribution pattern on autoradiographic sections. Moreover, results from μPET scans of (R)-[^{18}F]MH.MZ hint on improved molecular imaging characteristics compared with those of [^{18}F]MH.MZ. Therefore, (R)-[^{18}F]MH.MZ appears to be a highly potent and selective serotonergic PET ligand in small animals.
© 2010 Elsevier Inc. All rights reserved.

Keywords: MDL 100907; MH.MZ; PET; Fluorine-18; 5-HT2A receptor

1. Introduction

Several diseases and physiological processes, including appetite, emotion, changes in mood, depression, Alzheimer's disease and the regulation of the sleep/wake cycle, are involved in the serotonergic system [1–3]. In particular, many clinically approved atypical antipsychotic drugs are potent 5-HT$_{2A}$ receptors [4]. Therefore, in vivo positron emission tomography (PET) studies of the 5-HT$_{2A}$ receptor occupancy and availability would provide a significant advance in the understanding of the mentioned disorders and conditions. PET is an appropriate tool to measure noninvasively and repetitively various parameters like the binding potential, the receptor availability and uptake kinetics of radiotracers for neuroreceptors in vivo. Novel ^{18}F-labeled 5-HT$_{2A}$ antagonists would provide a significant advance in the field of molecular imaging of the serotonergic system as clinically used ligands to study the 5-HT$_{2A}$ receptor, like [^{18}F]altanserin or [^{11}]MDL 100907, have notable disadvan-

* Corresponding author. Tel.: +49 6131 39 25302; fax: +49 6131 39 24692.

E-mail address: frank.roesch@uni-mainz.de (F. Rösch).

[1] Both authors have equally contributed.

tages. [11C]MDL 100907 is a very specific high-affinity ligand for 5-HT$_{2A}$ receptors with limitations due to its slow kinetics and the short half-life of C-11 [5–7]. The binding of [18F]altanserin lacks specificity and in vivo stability [8,9].

Recently, we have reported the syntheses and first in vitro and in vivo evaluation of [18F]MH.MZ (**1**), an 18F-analog of MDL 100907 (Fig. 1) [9,10]. The novel labeling reaction route could possibly be a superior one compared to that of [18F]altanserin. In vivo and in vitro studies defined [18F]MH. MZ as a potent tracer to image the 5-HT$_{2A}$ receptor status via PET at least in rats [10].

With these encouraging results, a new series of MDL 100907 derivatives were synthesized aiming for even more selective reference ligands [11].

Due to experiments carried out in vitro, two novel and potent compounds [DD-1 and (R)-MH.MZ], displayed in Fig. 2, showed promising characteristics as high-affinity and selectivity ligands (Fig. 2) [11].

These results justified further experiments like in vitro autoradiography and in vivo microPET(μPET) experiments to prove the applicability of these two novel ligands. The manuscript reports on the labeling of DD-1 and (R)-MH.MZ with F-18 and their evaluation as potential new and improved 5-HT$_{2A}$ imaging agents in rats.

2. Methods and materials

2.1. Chemicals and reagents

All reagents and solvents used were of analytical-grade quality and purchased from Acros, Fluka or Merck. Unless otherwise noted, all chemicals were used without further purification.

2.2. High-performance liquid chromatography

2.2.1. Analytical HPLC

A high-performance liquid chromatography (HPLC) system was used equipped with a Sykam S 1100 solvent delivery system, S 8110 low pressure gradient mixer, Rheodyne 9725i inject valve; linear UVIS-205 absorbance detector; Axxiom Chromatography 900-200 Pyramid; Pyramid 2.07; loop: 20 μl.

2.2.2. Semipreparative HPLC

A HPLC system equipped with a Dionex P680A pump, a Raytest NaI scintillation counter (Gabi) and a Dionex UVD 170U (254 nm) absorbance detector was used.

Dionex Chromeleon software was used for UV-data analysis and Raytest Gina-star software was used for radioactivity detection.

2.3. Hardware

2.3.1. Imager

Autoradiographic images were analyzed via an image analyzer (FLA 7000 Fujifilm). Radioactive spots were detected using a Canberra Packard Instant Imager.

2.3.2. MicroPET

PET studies were performed with a Siemens MicroPET Focus 120 camera.

2.4. Animals

Male, 8-week-old, mature catheterized Sprague-Dawley (SD) rats obtained from the animal husbandry of the Johannes Gutenberg University of Mainz, Germany, were used for ex vivo distribution as well as for PET studies. All procedures were carried out in accordance with the European Communities Council Directive regarding care and use of animals for experimental procedures and were approved by local authorities of the state of Rhineland-Palatine.

2.5. Preparation of rat brain sections

Rats were narcotized with CO$_2$ and subsequently decapitated by a rodent guillotine. Brains were carefully removed from the skull and shortly rinsed in ice-cold 50 mM Tris/citrate (pH 7.4) buffer to remove hairs and blood. The brains were then frozen on a precooled −80°C cold steel plate. Brains were either stored in parafilm or in aluminum foil at −80°C or transferred to a Leica cryostate and kept in parafilm at −24°C for 30 min. After warming up to −24°C, brains were frozen onto an object carrier with tissue tack freezing medium in the desired orientation for either sagittal, coronal or transversal sectioning. Sections were cut at 14 μm thickness, knife angle of 5° and an object temperature of −13°C. Sections were melted onto super frosted glass slides (Menzel), air dried and were either used immediately or stored at −80°C until further use.

2.6. Radiochemistry

2.6.1. Preparation of the K[18F]F–K$_{222}$ complex

An anion exchange resin (Sep-Pak Light Waters Accell Plus QMA cartridge) was washed with aqueous 1 M K$_2$CO$_3$ (10 ml) and rinsed with water (20 ml) and CH$_3$CN (10 ml) by
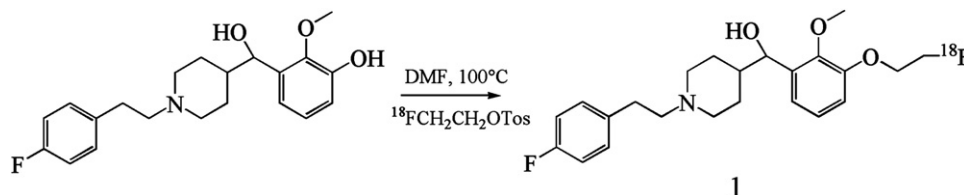
Fig. 1. Radiosynthesis of [18F]MH.MZ.
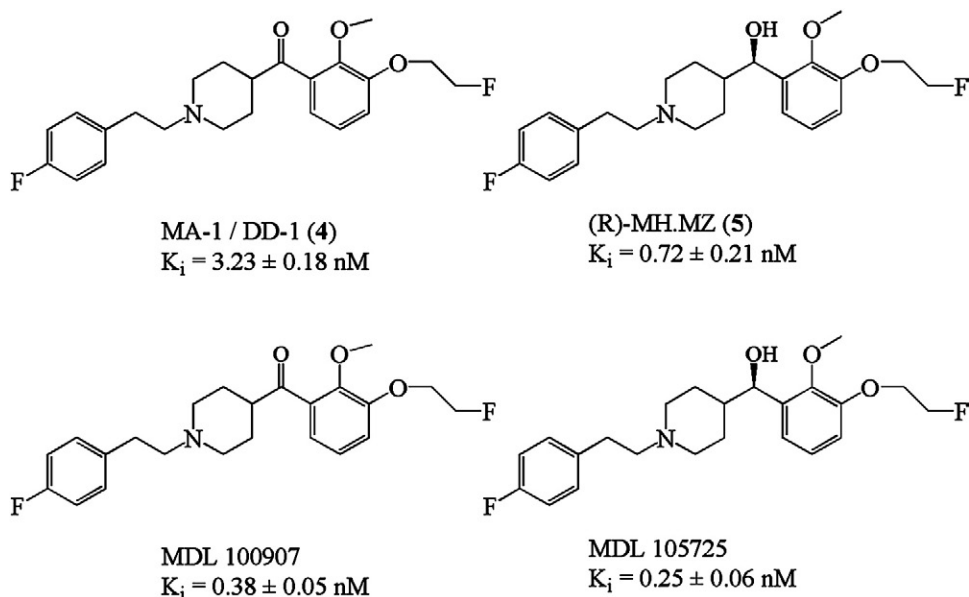
Fig. 2. Structures of new potent, selective [^{18}F]ligands of the 5-HT$_{2A}$ receptor, the original ^{11}C-labeled compound and its precursor MDL 105725 [11].

helium pressure (1.5–2 bar). Then the aqueous [^{18}F]fluoride solution was passed through this exchange resin. [^{18}F] Fluoride ions were then eluted from the resin using 15 μl of 1 M K$_2$CO$_3$ solution and 15 mg Kryptofix$_{222}$ (K$_{222}$: 4,7,13,16,21,24-hexaoxa-1,10diazabicyclo[8.8.8]hexacosane). The resulting solution was then gently concentrated to dryness at 90°C under a nitrogen stream for 15 min to give no-carrier-added K[^{18}F]F–K$_{222}$ complex as a white semi-solid residue.

2.6.2. Radiosynthesis of [^{18}F]FETos

The dried K[^{18}F]F–K$_{222}$ complex was then dissolved in 1 ml acetonitrile, and 4 mg (10 mmol) ethylenglycol-1,2-ditosylate was added and heated under stirring in a sealed vial for 3 min. Purification of the crude product was accomplished using HPLC (Lichrospher RP18-EC5; 250×10 mm; acetonitrile/water 50:50; flow rate: 5 ml/min; retention time [RT]: 8 min). After diluting the HPLC fraction containing the 2-[^{18}F]fluoroethyltosylate with water, the product was loaded on a Phenomenex strata-X 33-μm polymeric reversed-phase column, dried with nitrogen and eluted with 1 ml of tempered (40–50°C) DMSO.

2.6.3. General procedure of the synthesis of [^{18}F]FE-MDL 100907 derivatives

[^{18}F]FETos trapped on a Phenomenex strata-X 33-μm polymeric reversed-phase column was directly rinsed with 1 ml of tempered (40–50°C) DMSO into a vial with 3 mg precursor (8.3 μmol) and 1.5 μl 5N NaOH (7.5 μmol). The tube was placed in a heating block and stirred during the reaction time. The reaction vessel was then cooled to room temperature using an ice-water bath and quenched with 1 ml H$_2$O. The remaining radioactivity was measured, which was 90–95% of the initial radioactivity. The resulting reaction

mixture was analyzed by radio-TLC. The reaction yield was calculated from the TLC-radiochromatogram and defined as the ratio of radioactivity area of the ^{18}F-labeled compound over total fluorine-18.

(R)-[^{18}F]MHMZ: SiO$_2$-TLC, eluent: CHCl$_3$/MeOH/conz. NH$_3$, 8:1:0.2; (R)-[^{18}F]MHMZ: R_f=0.36, [^{18}F]FETos: R_f=0.95, [^{18}F]fluoride ion: R_f=0.0.
[^{18}F]DD-1: SiO$_2$-TLC: eluent: CHCl$_3$/MeOH, 20:1; [^{18}F]DD-1: R_f=0.72; [^{18}F]FETos: R_f=0.97; [^{18}F]fluoride ion: R_f=0.0.

2.6.4. Formulation

Formulation of the labeled product for evaluation studies was effected as follows: reactants and byproducts were separated from ^{18}F-tracers by semipreparative HPLC (μBondapak C$_{18}$ 7.8×300 mm column; RT; flow rate 8 ml/min).

(R)-[^{18}F]MHMZ: 0.05 M Na$_2$HPO$_4$ (pH 7.4 H$_3$PO$_4$)/ MeCN, 60:40 RT; [^{18}F]F$^-$=1.8 min; [^{18}F]FETos=4 min; (R)-[^{18}F]MHMZ=9.76 min; MDL 105725 (2)=4.85 min. [^{18}F]DD-1: 0.25 M NH$_4$Ac buffer (pH 5.6 acetic acid)/MeCN, 75:25; RT; [^{18}F]F$^-$=2.5 min; [^{18}F] FETos=11.54 min; [^{18}F]DD-1=21.73 min; [precursor (3)]=7.23 min.

The collected fraction containing the ^{18}F-labeled compound with water (4:1) was passed through a conditioned strataX-cartridge (1 ml EtOH, 1 ml H$_2$O) and washed with 10 ml H$_2$O. The ^{18}F-labeled compound was eluted with at least 1 ml of EtOH. Less than 8% of the total radioactivity was left on the cartridge. Finally, EtOH was removed in vacuo and the ^{18}F-labeled tracer was solved in 1 ml saline.

2.6.5. Quality control

The radiotracer preparation was visually inspected for clarity, absence of color and particulates. Chemical and radiochemical purities were also assessed on an aliquot by TLC analyses and by analytical HPLC (ET 250/8/4 Nucleosil 5 C_{18}).(R)-[^{18}F]MHMZ: see above.
[^{18}F]DD-1: NH$_4$Ac buffer (pH 5.6)/MeCN, 60:40; flow rate 1 ml/min; RT: [^{18}F]F$^-$=2.4 min; [^{18}F]FETos=16.34 min; [^{18}F]DD-1=24.63 min; [precursor (3)]=11.40.

Specific activity (A_s) of the radiotracer was calculated from three consecutive HPLC analyses (average) and determined as follows: the area of the UV absorbance peak of the ^{18}F-analogue of the ^{18}F-labeled tracer was integrated on the HPLC chromatogram and compared to a standard curve relating mass to UV absorbance.

2.7. In vitro autoradiography of rat brain slices with [^{18}F]DD-1 and (R)-[^{18}F]MH.MZ

Autoradiography experiments were carried out at room temperature in reaction buffer (50 mM Tris/HCl buffer, pH 7.4, containing 120 mM NaCl and 5 mM KCl) with ^{18}F-labeled compounds on ice. In the case of the challenge experiments (Section 3.2; Fig. 6), four competitors, ketanserin, fallypride, WAY 100635 and prazosin, were added in excess (10 μM).

Sections were washed 2×2 min in reaction buffer containing 0.01% Triton X-100 and 1×2 min in reaction buffer, shortly dipped into deionized water and quickly dried in a stream of cold air. Sections were exposed to Fuji phosphor screen for 3 h. Screens were read out with a Fuji FLA-7000 scanner. ^{18}F-Quantification was done after calibration by a standard curve which was obtained by a dilution series of an ^{18}F-solution. Calibration was repeated for each fresh radiotracer synthesis. Calibration, quantification and data evaluation were done with the Fujifilm MultiGauge image analysis software.

2.8. In vivo PET studies of (R)-[^{18}F]MH.MZ

Positron emission tomography scans were performed with a Siemens/Concorde Microsystems microPET Focus 120 small animal PET (μPET) scanner. Eight-week-old male Sprague-Dawley rats (weight: 220–325 g) were obtained from the animal husbandry of the Johannes Gutenberg University of Mainz. Animals were anesthetized with a combination of xylazine (Rompun) (2%) and ketamine (Ketavet) (10%) by intraperitoneal injection of 1.1 ml/kg. Rats were placed in supine position on the scanner bed and fixed with adhesive strips. Listmode acquisition was started with the tracer injection of 15 MBq (specific activity: 35–45 GBq/μmol). The ^{18}F-labeled tracer was applied via intravenous injection into the femoral vein catheter. Then, catheters were flushed with 0.25 ml isotonic 0.9% NaCl solution.

After the dynamic recordings, a transmission scan for attenuation correction was carried out using a ^{57}Co point source. Listmode acquisition was histogrammed into 25 frames. The frame duration increased progressively from 20 s to 5 min resulting in a total scanning time of 90 min. Finally, images were reconstructed with scatter and attenuation correction using a 3D maximum a posteriori (MAP) algorithm with 18 iterations and regularization parameter of 0.002.

Images were scaled as standardized uptake values (SUVs) which is defined as: activity concentration in becquerel per milliliter×body weight in grams/injected dose in becquerel. Kinetic modeling and image quantification were carried out using the PMOD software package. First, the images were transformed into standardized views according to the Paxinos orientation. A volume-of-interest (VOI) template comprising the frontal cortex, cortex [motor and somatosensory cortex (parietal and temporal cortex)] and the cerebellum was defined on transaxial slices using an integral image between 60 and 90 min postinjection reflecting specific binding of the tracer. Time–activity curves (TAC) were derived from dynamic kinetics. Assuming negligible receptor density, the cerebellum was used as a reference region. Binding potential (BP) was calculated using the TAC and the simplified reference tissue model.

3. Results and discussion

3.1. Radiochemistry

Precursors and reference compounds were synthesized as previously described [11]. Radioactive labeling was carried out similar to the reported synthesis of [^{18}F]MH.MZ [9,10]. Thereby, necessary [^{18}F]FETos synthon production was performed in an automated module according to Bauman et al. [12] and used for [^{18}F]fluoroalkylation resulting in (R)-[^{18}F]MH.MZ and [^{18}F]DD-1 (Fig. 3).

[^{18}F]Fluoroalkylation of the precursor (2) was optimized only due to temperature variations resulting in radiochemical yields >70%. Labeling kinetics were compared with those reported for [^{18}F]MH.MZ, whereas the [^{18}F]alkylation of the enantioselective precursor (R)-MDL 105725 (3) was carried out using exactly the same reaction conditions as for its racemic analog. Used parameters enable radiochemical yields of about 80%. Final reaction conditions were 100°C, 15 min reaction time, 7 mmol precursor, 7 mmol 5N NaOH and dry DMSO (Fig. 4).

The final formulation of the injectable solution including a semipreparative HPLC took no longer than 100 min for all compounds and provided ^{18}F-labeled tracers with a radiochemical purity of >96% and a chemical purity of >98% indicated by HPLC analyses. Typical specific activities (A_s) are between 35 and 45 GBq/μmol. Thereby, amounts of ~3 GBq of [^{18}F]fluorine were used as starting radioactivity.
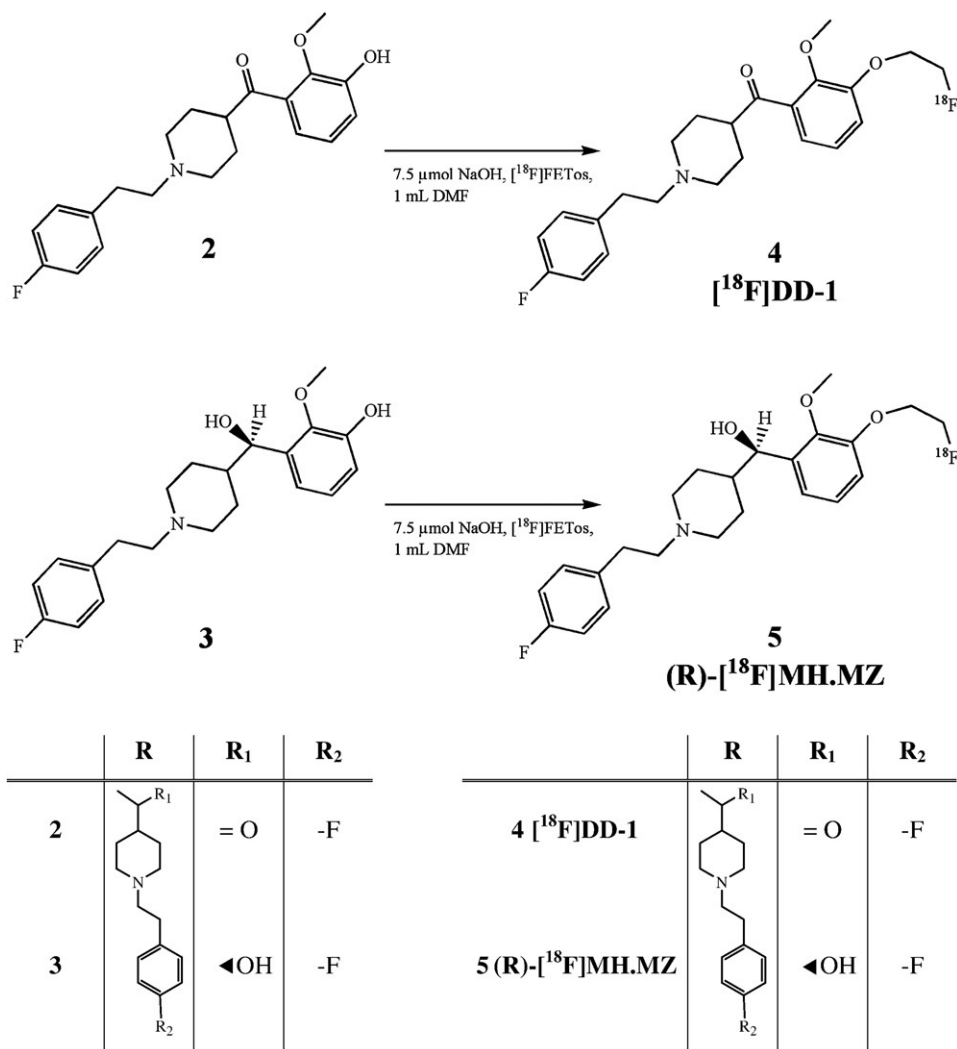
Fig. 3. Syntheses of [^{18}F]DD-1 and (R)-[^{18}F]MH.MZ.
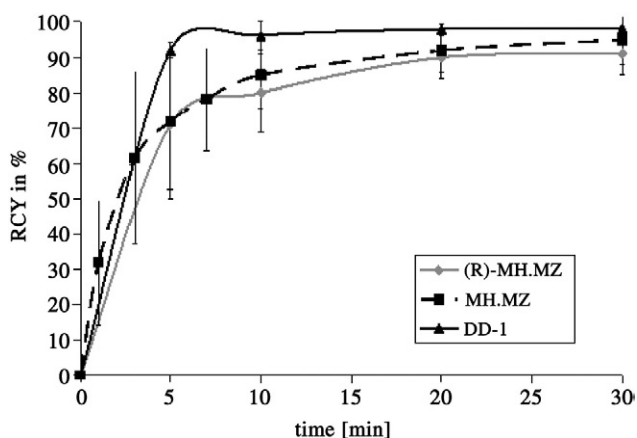
Fig. 4. ^{18}F-Fluoroalkylation of 7 mmol precursor at 100°C using DMF and 7 mmol 5N NaOH yielding [^{18}F]MH.MZ, [^{18}F]DD-1 and (R)-[^{18}F]MH.MZ.

The new ^{18}F-labeled compounds could be obtained as an injectable solution in an overall radiochemical yield of about 40% referred to the starting activity of ^{18}F-fluoride. This is very similar to the radiosynthesis of [^{18}F]altanserin, which takes 75 to 100 min and results in a radiochemical yield of 30–50% [13].

3.2. In vitro autoradiography

Autoradiographic images obtained with (R)-[^{18}F]MH.MZ (5) and [^{18}F]DD-1 (4) showed accumulation of radioactivity in known 5-HT$_{2A}$ receptor regions in rat brain slices at equal A_s of 30 GBq/μmol (Fig. 5).

Excellent visualization was obtained by (R)-[^{18}F]MH. MZ. These data are in accordance with the known distribution of [^{3}H]MDL 100907 [14,15] and [^{18}F]MH.MZ [9] in the rat brain.

Due to the higher 5-HT$_{2A}$ binding of (R)-MH.MZ (K_i=0.72 nM) compared to MH.MZ (K_i=3.0 nM), this enantioselective tracer should be more valuable in PET experiments concerning the possibly improved binding
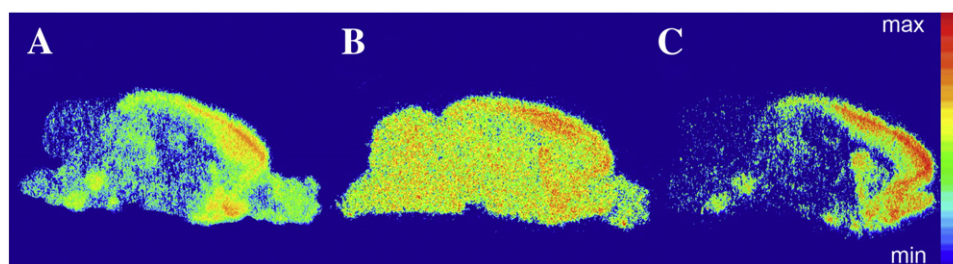
Fig. 5. Images of an autoradiography of [^{18}F]MH.MZ (left) , (R)-[^{18}F]MH.MZ (right) and [^{18}F]DD-1 (middle) show high specific binding for the MH.MZ analogues and less for [^{18}F]DD-1 at 14-μm-thick rat brain sections; major binding was detected in lamina V of the frontal cortex.

potential (BP) and the regional cortex-to-cerebellum ratio within the brain.

Visualization by [^{18}F]DD-1 showed less specific binding (Fig. 5). Indeed, reduced binding characteristics could be expected due to its decreased affinity compared to (R)-[^{18}F]MH.MZ (Table 1), but were not necessarily likely for [^{18}F]DD-1 compared to its [^{18}F]MH.MZ analogue (Table 1). In addition, selectivity of [^{18}F]DD-1 showed no intense alteration compared to that of MH.MZ [11]. Therefore, the observed properties are most probably due to the increased lipophilicity of [^{18}F]DD-1 (MH.MZ: log$P$=2.80±0.06; DD-1: log$P$=3.08±0.1) [11].

Competition autoradiography experiments (Fig. 6) were conducted with the new enantioselective tracer to prove its potential as a PET imaging agent. Thereby, 1 nM of (R)-[^{18}F]MH.MZ and 10 μM of ketanserin, fallypride, WAY 100635 and prazosin were used in these competition assays. High specificity of (R)-[^{18}F]MH.MZ toward the 5-HT$_{2A}$ receptors was obtained as expected because of the affinity and selectivity determined by radioligand binding assays through the NIMH Psychoactive Drug Screening Program (PDSP) [11].

Total displacement could be observed with ketanserin as a known 5-HT$_{2A}$ receptor ligand, whereas no displacement could be detected with WAY 100635, a 5-HT$_{1A}$ antagonist, and prazosin, an α$_1$ ligand. Another displacement could only be detected with fallypride. However, co-incubation of fallypride led to a displacement of 25±8% (n=4) of total binding in the frontal cortex as well as in the caudate–putamen, which does not imply that [^{18}F]MH.MZ recognizes D$_2$/D$_3$ receptors but might rather be explained by the known cross affinity of fallypride to 5-HT$_2$ receptors (Fig. 6) [16]. These results are very similar to those observed with

the racemic analogue, [^{18}F]MH.MZ [9] and [^{3}H]MDL 100907 [14,17]. Especially, the advantage of MDL 100907 over altanserin regarding the D$_2$ affinity could be retained by both the racemic and its enantioselective ligand (R)-[^{18}F]MH.MZ. Herth et al. [9] demonstrated this superior in vitro behavior of [^{18}F]MH.MZ by autoradiographic experiments. Whereas [^{18}F]altanserin showed a strong D$_2$ binding within the striatum, no specific accumulation could be observed either by [^{18}F]MH.MZ [9] or by (R)-[^{18}F]MH.MZ (Fig. 5) in these regions.

Binding parameters of (R)-[^{18}F]MH.MZ of cortex-to-cerebellum ratios of the rat brain obtained with autoradiography assays at equal levels of specific activities at sagittal sections are shown in Table 1 and compared with the binding parameters of [^{18}F]MH.MZ and [^{3}H]MDL 100907 [9]. Binding in the cerebellum was at the level of nonspecific binding, so levels of binding in different brain regions are also given relative to that brain area. However, as a matter of fact, (R)-[^{18}F]MH.MZ showed region-to-cerebellum ratios almost twice as high as compared with [^{18}F]MH.MZ. Results of [^{18}F]DD-1 were not evaluated due to its unfavorable distribution pattern.

In conclusion, the results suggest that the nonspecific binding associated with these radiotracers is low for [^{18}F]MH.MZ and (R)-[^{18}F]MH.MZ and moderate to low for [^{18}F]DD-1 (Fig. 4). [^{18}F]MH.MZ and (R)-[^{18}F]MH.MZ could possibly be useful as ^{18}F-labeled tracers for imaging the 5-HT$_{2A}$ receptor in vivo by PET experiments. Especially, (R)-[^{18}F]MH.MZ could improve binding characteristics such as BP or regional distribution expressed as cortex-to-cerebellum ratios due to its higher affinity. In comparison to [^{3}H]MDL 100907 and [^{18}F]altanserin, (R)-[^{18}F]MH.MZ and also [^{18}F]MH.MZ are in no way inferior in terms of specificity for 5-HT$_{2A}$ receptors and region cortex-to-cerebellum ratios [9,14,17].

3.3. In vivo PET experiments

Due to the relatively moderate binding characteristics of [^{18}F]DD-1, only PET scans with (R)-[^{18}F]MH.MZ were performed, expecting better in vivo results compared to with its racemic derivative [^{18}F]MH.MZ. Dynamic images were analyzed with pixel-wise modeling computer software (PMOD; Zurich, Switzerland). For illustrative purposes,

Table 1
Binding parameters obtained with (R)-[^{18}F]MH.MZ and [^{18}F]MH.MZ from binding in vitro autoradiographic experiments at 14-μm-thick sagittal sections of the rat brain

	n	(R)-[^{18}F]MH.MZ	[^{18}F]MH.MZ	[^{3}H]MDL 100907
		Region/cerebellum ratio		
Lamina V	4	91.8±0.5	59.5±2.8	105.5±0.8
Frontal cortex	4	57.5±3.2	31.4±1.3	54.4±4.2

Values are shown as means±S.E.M.
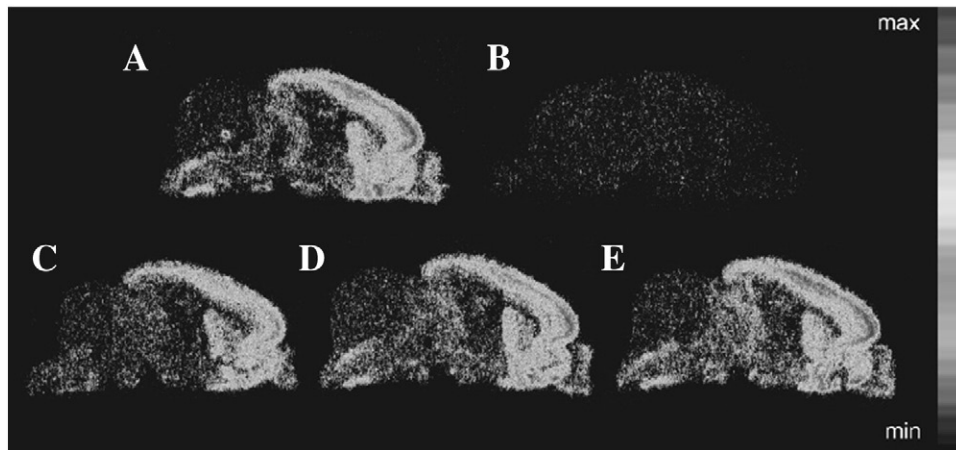
Fig. 6. Sagittal autoradiographies on 14-μm-thick rat brain sections with (R)-[^{18}F]MHMZ at a concentration of 1 nM (K_i=0.72 nM for 5-HT$_{2A}$). (A) Total binding, (B) nonspecific binding measured in the presence of 10 μM ketanserin, (C) co-incubation with 10 μM fallypride, (D) co-incubation with 10 μM WAY 100635, (E) co-incubation with 10 μM prazosin.

an integral image between 60 and 90 min after tracer injection is displayed in Fig. 7, whereby the last 30 min of the dynamics reflects the specific binding of (R)-[^{18}F]MH. MZ. Images are shown in horizontal orientation with a slice thickness of 0.8 cm. False color-coded images in Fig. 7A display horizontal slices through the rat brain from top (1) to bottom (12), whereas Fig. 7B shows a representative horizontal slice through the cortex, the frontal cortex and the cerebellum area.

These PET images clearly visualize the binding of (R)-[^{18}F]MH.MZ in the frontal cortex known to possess high availability of 5-HT$_{2A}$ receptors, whereas the cerebellum,

which is believed to be devoid of 5-HT$_{2A}$ receptors, is at background level [14]. Results are very similar to those obtained by its racemic analogue [^{18}F]MH.MZ.[9]

Fig. 8 shows a representative time–activity curve (TAC) of a total binding study of (R)-[^{18}F]MH.MZ which included four animals. Results are given as standardized uptake value (SUV) (% injected dose in becquerel per milliliter×animal weight in grams). Uptake of (R)-[^{18}F]MH.MZ between 60 and 90 min is more than 150% higher in cortical regions than in the cerebellum, whereas the uptake of [^{18}F]MH.MZ is only 50% higher in these regions [9]. The binding potential (BP) of (R)-[^{18}F]MH.MZ was determined to be 2.6 for the
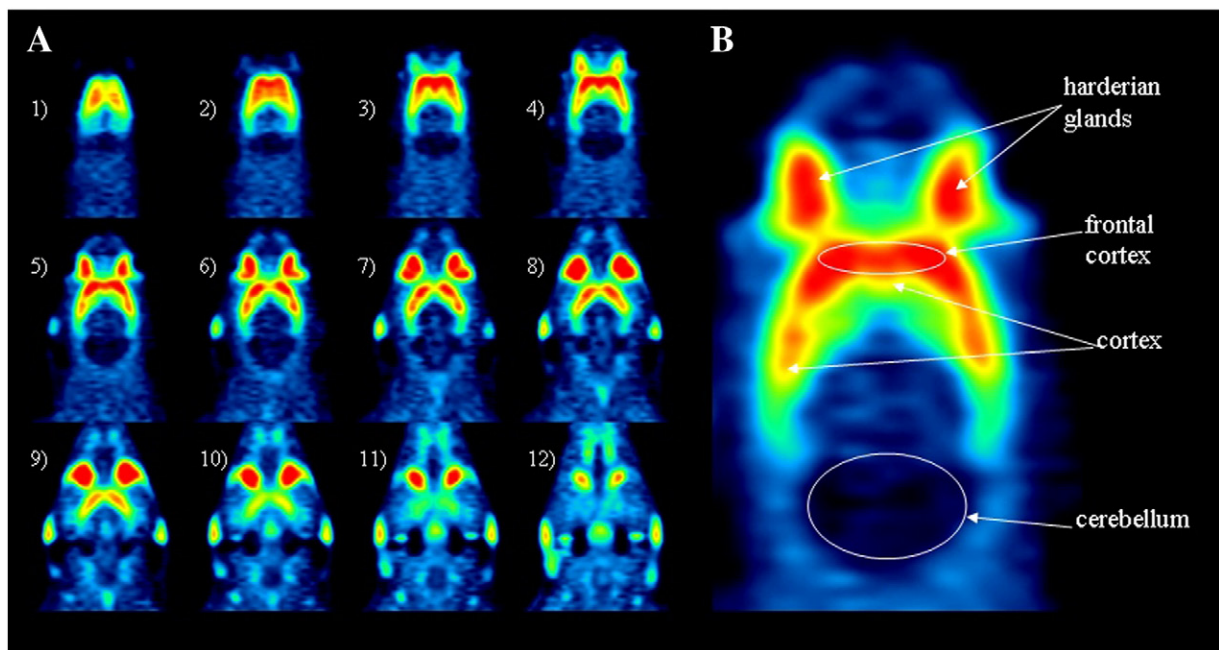
Fig. 7. MicroPET images of (R)-[^{18}F]MH.MZ binding in horizontal orientation. (A) Horizontal slices from top (1) to bottom (12). (B) Representative horizontal slice through the cortex, the frontal cortex and the cerebellum showing highest specific binding in the frontal cortex and a high nonspecific binding in the harderian glands. Uptake in the cerebellum was at background level.
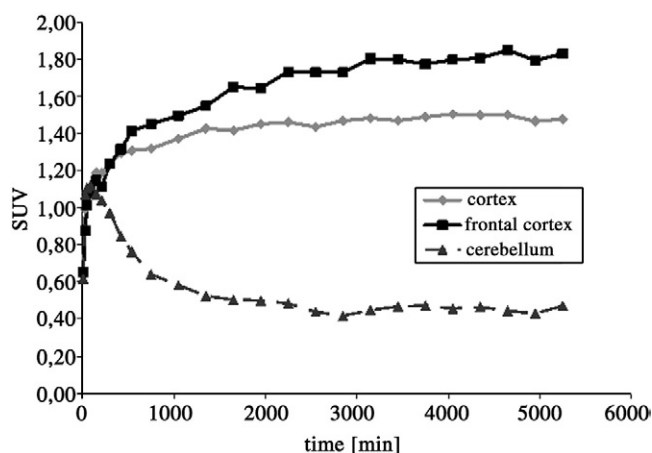
Fig. 8. Representative time–activity curve (TAC) of μPET experiments of (R)-[18F]MH.MZ in SD rats. The graph shows the results of a total binding study. Results are given as SUV (% injected dose in becquerel per milliliter×animal weight in grams).

frontal cortex region and to be 2.2 for the cortex (n=4) using a simplified reference tissue model and the PMOD software, whereas the BP for its racemic derivative, [18F]MH.MZ, was only determined to be 1.45 in the frontal cortex [9]. Cerebellum uptake is used as a reference region and is used instead of a plasma input curve. The time–activity curve shows the uptake in the frontal cortex, in the cortex as well as in the cerebellum.

The region-to-cerebellum ratios between 60 and 90 min obtained by μPET studies (n=4) are displayed in Table 2. An improved ratio of 3.3 was found for (R)-[18F]MH.MZ compared to the value of 2.7 for its racemic analogue [18F] MH.MZ. The ratio for the frontal cortex was also improved to be 3.9. According to the time–activity curves (TAC) displayed in Fig. 8, steady state appears to be reached between 28 and 35 min postinjection and the specific binding remains very constant over 60 min. This is identical with that observed with [18F]MH.MZ.

In comparison, [11C]MDL 100907 region-to-cerebellum ratios were shown to be slightly lower compared to those of (R)-[18F]MH.MZ (Table 2) [18]. Therefore, the enantioselective derivative (R)-[18F]MH.MZ is probably the more valuable tracer for molecular imaging of the 5-HT₂A receptor system by PET at least in rats.

These observations demonstrate the superior μPET behavior of (R)-[18F]MH.MZ in comparison to [18F] altanserin at least in rats. [18F]Altanserin, the most used PET ligand to image the 5-HT₂A receptor status in human, has recently been shown to be a strong substrate of one efflux transporter in rats, namely, P-glycoprotein (P-gp). Ex vivo as well as in vivo studies in rats showed that altanserin has a limited brain uptake in rats. Consequently, its binding potential (BP) is highly variable [19].

Moreover, we studied the in vivo stability profile of (R)-[18F]MH.MZ. For the analysis of preliminary in vivo metabolism of (R)-[18F]MH.MZ in brain and blood, samples

were treated as described [10]. Metabolite and intact tracer were analyzed by radio-TLC (CHCl₃/MeOH 5:2). The tracer underwent fast metabolism comparable to its racemic derivative [10]. Only one polar metabolite was found in plasma, and the percentage of unmetabolized fractions was 40%, 35%, 13% and 5% at 5, 10, 30 and 60 min, respectively. In comparison, Scott and Heath [20] investigated the in vivo metabolism of MDL 100907 and its main metabolite MDL 105725. These pharmacokinetic studies demonstrated that MDL 100907 undergoes a rapid first-pass metabolism [20]. This is very similar to our observed results. Radio-TLC analyses showed nonmetabolized (R)-[18F]MH.MZ within the brain at 60 min postinjection and almost no radioactive metabolite within the brain, as already observed for the racemate [10]. These findings could also be observed for MDL 100907 by Scott and Heath [20]. MDL 100907 as MH.MZ does not appear to be metabolized within the brain [10,20].

In summary, maintained data for (R)-[18F]MH.MZ are in accordance with those of [18F]MH.MZ and MDL 100907 [20].

4. Conclusion

Two new 5-HT₂A affine tracers, [18F]DD-1 (Kᵢ=3.23 nM) and (R)-[18F]MH.MZ (Kᵢ=0.72 nM), were 18F-fluoroalkylated by the secondary synthon [18F]FETos in radiochemical yields of >70%. The final formulation of the injectable solution including [18F]FETos synthesis took no longer than 100 min for the two compounds. The overall RCY was about 40%. It provided 18F-labeled compounds with a purity >96% and a typical specific activity of 35–40 GBq/μmol with a starting radioactivity of ~3 GBq of [18F]fluorine.

Autoradiographic images of **5** and **4** showed excellent visualization of the 5-HT₂A receptor for (R)-[18F]MH.MZ and less specific binding for [18F]DD-1 in rat brain slices. This is reasonable for (R)-[18F]MH.MZ due to its increased affinity, but unexpected for [18F]DD-1. The reduced binding for [18F]DD-1 may be explained by its decreased affinity compared to (R)-[18F]MH.MZ; nonetheless, it is unexpected when comparing its affinity with the racemic derivative [18F]MH.MZ. In addition, selectivity of [18F]DD-1 showed no intense alteration compared to that of MH.MZ. Therefore, the observed properties are most probably due to the increased lipophilicity of [18F]DD-1.

Table 2
Region to cerebellum ratios of (R)-[18F]MH.MZ between 60 and 90 min and [11C]MDL 100907 between 20 and 60 min maintained by μPET studies in rat brains (n=4)

Region	(R)-[18F]MH.MZ	[11C]MDL 100907[18]
Cortex	3.3±0.2	–
Frontal cortex	3.9±0.1	2.9

Competition autoradiography experiments were conducted with the new enantioselective tracer to prove its selective binding characteristics. Cortex-to-cerebellum ratios of (R)-[^{18}F]MH.MZ binding were almost twice as high as compared to [^{18}F]MH.MZ binding. Equal levels of specific activities were used for these experiments.

Results from μPET scans of (R)-[^{18}F]MH.MZ hint on significantly improved molecular imaging characteristics compared with those of [^{18}F]MH.MZ due to the higher 5-HT$_{2A}$ binding of (R)-MH.MZ (K_i=0.72 nM) compared to MH.MZ (K_i=3.0 nM). High uptake could be demonstrated in cortex regions. The binding potential of (R)-[^{18}F]MH.MZ was determined to be 2.2 in the cortex and 2.6 in the frontal cortex (n=4), whereas the cortex-to-cerebellum ratio was determined to be 3.3 at steady state in the cortex and 3.9 in the frontal cortex (60–90 min, n=4). All values represent an important improvement compared to those obtained with [^{18}F]MH.MZ [9].

Therefore, the enantioselective derivative (R)-[^{18}F]MH.MZ is probably the more valuable tracer for molecular imaging of the 5-HT$_{2A}$ receptor system by PET.

Acknowledgments

References

[1] Smith GS, Price JC, Lopresti BJ, Huang Y, Simpson N, Holt D, et al. Test–retest variability of serotonin 5-HT$_{2A}$ receptor binding measured with positron emission tomography and [^{18}F]altanserin in the human brain. Synapse 1998;30:380–92.

[2] Naughton M, Mulrooney JB, Leonard BE. A review of the role of serotonin receptors in psychiatric disorders. Hum Psychopharmacol 2000;15:397–415.

[3] Davis KL, Charney D, Coyle JT, Nerneroff C. Neuropsychopharmacology: the fifth generation of progress. New York: Raven Press; 2002.

[4] Jones BE, Kryger MH, Roth T, Dement WC. Principles and practice of sleep medicine. Philadelphia: W.B. Saunders Company; 2000. p. 134–54.

[5] Hall H, Farde L, Halldin C, Lundkvist C, Sedvall G. Autoradiographic localization of 5-HT$_{2A}$ receptors in the human brain using [^{3}H]M100907 and [^{11}C]M100907. Synapse 2000;38:421–31.

[6] Watabe H, Channing MA, Der MG, Adams HR, Jagoda E, Herscovitch P, et al. Kinetic analysis of the 5-HT$_{2A}$ ligand [^{11}C]MDL 100,907. J Cereb Blood Flow Metab 2000;20:899–909.

[7] Ito H, Nyberg S, Halldin C, Lundkvist C, Farde L. PET imaging of central 5-HT$_{2A}$ receptors with carbon-11-MDL 100907. J Nucl Med 1998;39:208–14.

[8] Tan P, Baldwin RM, Fu T, Charney DS, Innis RB. Rapid synthesis of F-18 and H-dual labeled altanserin, a metabolically resistant PET ligand for 5-HT$_{2A}$ receptor. J Labelled Compd Radiopharm 1999;42:457–67.

[9] Herth MM, Debus F, Piel M, Palner M, Knudsen GM, Lüddens H, et al. Total synthesis and evaluation of [^{18}F]MH.MZ. Bioorg Med Chem Lett 2008;18:1515–9.

[10] Herth MM, Piel M, Debus F, Schmitt U, Lüddens H, Rösch F. Preliminary in vivo and ex vivo evaluation of the 5-HT$_{2A}$ imaging probe [^{18}F]MH.MZ. Nucl Med Biol 2009;36:447–54.

[11] Herth MM, Kramer V, Piel M, Palner M, Riss PJ, Knudsen GM, et al. Synthesis and in vitro affinities of various MDL 100907 derivatives as potential ^{18}F-radioligands for 5-HT$_{2A}$ receptor imaging with PET. Bioorg Med Chem 2009;17:2989–3002.

[12] Bauman A, Piel M, Schirrmacher R, Rösch F. Efficient alkali iodide promoted ^{18}F-fluoro-ethylations with 2-[^{18}F]fluoroethyl tosylate and 1-bromo-2-[^{18}F]fluoroethane. Tetrahedron Lett 2003;44:9165–7.

[13] Lemaire C, Cantineau R, Guillaume M, Plenevaux A, Christiaens L. Fluorine-18-altanserin: a radioligand for the study of serotonin receptors with PET: radiolabeling and in vivo biologic behavior in rats. J Nucl Med 1991;32:2266–72.

[14] Lopez-Gimenez JF, Mengod D, Palacios JM, Vilario MT. Selective visualization of rat brain 5-HT$_{2A}$ receptors by autoradiography with [^{3}H]MDL 100,907. Naunyn-Schmiedeberg's Arch Pharmacol 1997;356:446–54.

[15] Lundkvist C, Halldin C, Ginovart N, Swahn CG, Carr AA, Brunner F, et al. [^{11}C]MDL 100907, a radioligand for selective imaging of 5-HT (2A) receptors with positron emission tomography. Life Sci 1996;58:187–92.

[16] Stark D, Piel M, Hübner H, Gmeiner P, Gründer G, Rösch F. In vitro affinities of various halogenated benzamide derivatives as potential radioligands for non-invasive quantification of D$_2$-like dopamine receptors. Bioorg Med Chem 2007;15:6819–29.

[17] Johnson M. [^{3}H]MDL 100907: a selective 5-HT$_{2A}$ receptor ligand. Naunyn-Schmiedeberg's Arch Pharmacol 1996;354:205–10.

[18] Hirani E, Sharp T, Sprakes M, Grasby P, Hume S. Fenfluramine evokes 5-HT$_{2A}$ receptor-mediated responses but does not displace [11C]MDL 100907: small animal PET and gene expression studies. Synapse 2003;50:251–60.

[19] Palner M, Syvänen S, Kristoffersen US, Gillings N, Kjaer A, Knudsen GM. The effect of a P-glycoprotein inhibitor on rat brain uptake and binding of [^{18}F]altanserin: a micro PET study. (abstract)Brain and Mind Forum 2007.

[20] Scott DO, Heath TG. Investigation of the CNS penetration of a potent 5-HT$_{2A}$ receptor antagonist (MDL 100,907) and an active metabolite (MDL 105,725) using in vivo microdialysis sampling in the rat. J Pharmaceut Biomed Anal 1998;17:17–25.